Insect science

*Insect Science* (2022) 29, 453–466, DOI 10.1111/1744-7917.12944

ORIGINAL ARTICLE

# Involvement of *CYP347W1* in neurotoxin 3-nitropropionic acid-based chemical defense in mustard leaf beetle *Phaedon cochleariae*

Nanxia Fu[1,2], Tobias Becker[1], Wolfgang Brandt[3], Maritta Kunert[1,4], Antje Burse[1,5] and Wilhelm Boland[1]

[1]*Department of Bioorganic Chemistry, Max Planck Institute for Chemical Ecology, Jena, Germany;* [2]*Key Laboratory of Tea Biology and Resource Utilization, Tea Research Institute, Chinese Academy of Agricultural Sciences, Hangzhou, China;* [3]*Department of Bioorganic Chemistry, Leibniz Institute of Plant Biochemistry, Halle (Saale), Germany;* [4]*Department of Natural Product Biosynthesis, Max Planck Institute for Chemical Ecology, Jena, Germany and* [5]*Department of Medical Technology and Biotechnology, Ernst Abbe Hochschule Jena, Jena, Germany*

**Abstract** Chrysomelina beetlesstore 3-nitropropionic acid in form of a pretoxin, isoxazolin-5-one glucoside-conjugated ester, to protect themselves against predators. Here we identified a cytochrome P450 monooxygenase, *CYP347W1*, to be involved in the production of the 3-nitropropionic acid moiety of the isoxazolin-5-one glucoside ester. Knocking down *CYP347W1* led to a significant depletion in the concentration of the isoxazolin-5-one glucoside ester and an increase in the concentration of the isoxazolin-5-one glucoside in the larval hemolymph. Enzyme assays with the heterologously expressed *CYP347W1* showed free $\beta$-alanine was not the direct substrate. Homology modeling indicated that $\beta$-alanine-CoA ester can fit into *CYP347W1*'s active site. Furthermore, we proved that *Phaedon cochleariae* eggs are not able to de novo synthesize 3-NPA, although both isoxazolin-5-one glucoside and its 3-NPA-conjugated ester are present in the eggs. These results provide direct evidence for the involvement of *CYP347W1* in the biosynthesis of a *P. cochleariae* chemical defense compound.

**Key words** chemical defense; isoxazolin-5-one glucoside; isoxazolin-5-one glucoside ester; leaf beetles; P450; 3-nitropropionic acid (3-NPA)

## Introduction

The neurotoxin 3-nitropropionic acid (3-NPA) and its derivatives are a group of structurally related and toxicologically important nitrogen-containing natural compounds. The intoxication by 3-NPA and its derivatives has caused severe losses of domestic livestock (Williams *et al*., 1969; Williams & James, 1975; James *et al*., 1980).

Correspondence: Nanxia Fu, Antje Burse, and Wilhelm Boland, Department of Bioorganic Chemistry, Max Planck Institute for Chemical Ecology, Hans Knöll Straße 8, 07745 Jena, Germany. Email: funanxia@tricaas.com; antje.burse@eah-jena.de; Boland@ice.mpg.de

Similar 3-NPA intoxication incidents were also reported from humans due to ingestion of moldy sugarcanes (Liu *et al*., 1992; Hamilton *et al*., 2000). Due to its similarity to succinic acid, 3-NPA acts as a suicide inhibitor to succinate dehydrogenase (EC No. 1.3.99.1) and can block the electron transport chain that is essential for all living cells (Huang *et al*., 2006). In mammals, the blockage of ATP production caused by 3-NPA leads to neurodegeneration with symptoms similar to those found in the patients with Huntington's disease (Tunez *et al*., 2010).

Since its first discovery as a glucoside in the tropical plant *Hiptage madablota* Geartn, the occurrence of 3-NPA and its derivatives has been identified in an increasing number of species from both fungi and leguminous

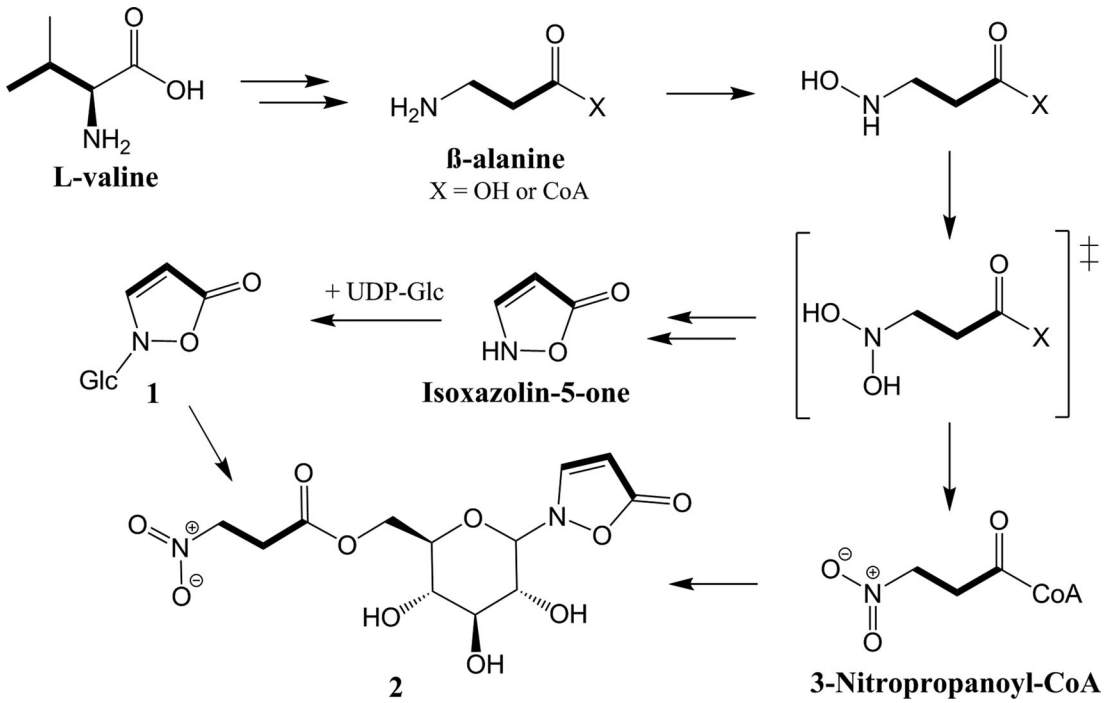


**Fig. 1** The proposed biosynthetic pathway of compounds 1 and 2 in *P. cochleariae* (adopted from Becker *et al*., 2016).

plants (Baxter & Greenwood, 1986; Baxter *et al*., 1992; Hamilton *et al*., 2000; Anderson *et al*., 2005). In insects, adults of Chrysomelina leaf beetles were also reported to store the 3-NPA containing pretoxin, isoxazolin-5-one glucoside derived ester, to protect themselves from natural enemies (Baxter & Greenwood, 1986; Randoux *et al*., 1991). Recent studies have shown that the isoxazolin-5-one glucoside (compound 1) and the corresponding 3-NPA-conjugated ester (compound 2) (Fig. 1) coexist in all the different life stages of Chrysomelina leaf beetles, and are present as major secondary metabolites in eggs, in larval hemolymph, in pupal and adults' hemolymph and defensive secretions (Becker *et al*., 2016; Pauls *et al*., 2016). Since compound 2 showed a highly deterrent effect to the ant *Myrmica rubra*, it was considered to constitute a cornerstone of the chemical defense arsenal for the Chrysomelina beetles against predatory ants, whilst compound 1 acted mainly as a precursor to conjugate the poisonous 3-NPA to avoid self-intoxication (Pasteels *et al*., 1986).

With stable isotope-labeled precursor feeding experiments, the biosynthesis of compounds 1 and 2 in leaf beetles of the Chrysomelina subtribe have been studied in detail. Unlike the leguminous plants and fungi, leaf beetles, for example, *P. cochleariae*, utilize L-valine instead of L-aspartic acid or malonate as the precursor for the production of compounds 1 and 2 (Baxter *et al*., 1994; Robert & Christian, 2007; Su *et al*., 2008; Becker *et al*., 2016; Huang *et al*., 2016). The proposed biosynthetic pathway of compounds 1 and 2 in larvae of the Chrysomelina leaf beetles is shown in Fig. 1 (Becker *et al*., 2016). The backbones of both compounds 1 and 2 are derived from $\beta$-alanine, an amino acid that can be either sequestered from host plants or synthesized by the degradation of some essential amino acids, for example L-valine via propanoyl-CoA. By consecutive oxidations at the amino group, $\beta$-alanine is converted further into 3-NPA and isoxazolin-5-one, respectively. The substitution of the diphosphate group of $\alpha$-UDP-glucose with isoxazolin-5-one generates compound 1, which is further conjugated with the 3-NPA moiety, yielding compound 2 (Randoux *et al*., 1991; Becker *et al*., 2016). Even though the sequential reactions have been chemically proposed, the enzymes that are involved in the pathway remain to be identified.

As the proposed biosynthetic pathway of both compounds 1 and 2 in *P. cochleariae* includes two sequential oxidations at the nitrogen atom of $\beta$-alanine and a ring formation reaction, Cytochrome P450s (CYPs) are proposed to catalyze these reactions. CYPs are a superfamily of heme-thiolate monooxygenases, and have been identified in all kingdoms of life, including the viruses (Lamb *et al*., 2009). One of the most fundamental reactions that P450s catalyze is to introduce one oxygen atom into the nonactivated carbon-hydrogen bond

(Montellano, 2010; Greule *et al*., 2018). Additionally, P450s were reported to mediate a diverse array of other oxidations as well as some novel reactions, for example, the oxygenation at heteroatoms, ring formations, and so on (Guengerich, 2001; Lamb & Waterman, 2013). However, a correlation between the biosynthetic reactions in the pathway leading up to compound 2 and cytochrome P450 monooxygenases has not been demonstrated so far.

To investigate whether *P. cochleariae* harbor P450(s) that participate(s) in the production of compound 1 and its 3-NPA-conjugated ester 2, we used a combination of double-stranded RNA (dsRNA) mediated RNA interference (RNAi) and high performance liquid chromatography-mass spectrometry (HPLC) to screen the P450 candidates. Herein, we report the identification of one cytochrome P450, *CYP347W1*, which was proven to play an important role in the biosynthesis of the 3-NPA moiety of compound 2. In vitro enzyme assays using successfully heterologously expressed CYP347W1 showed it could not convert free $\beta$-alanine. Homology model indicated that $\beta$-alanine-CoA ester is a promising substrate for CYP347W1. Furthermore, our results showed that the eggs are unable to synthesize the 3-NPA moiety de novo.

## Materials and methods

### *Leaf beetles*

The mustard leaf beetle, *P. cochleariae*, was reared in the lab continually on Chinese cabbage *Brassica oleracea* convar. *capitata* var. *alba* (Gloria F1) in a 16 h light to 8 h dark cycle at 15°C ± 2°C. *Chrysomela populi* (L.) were collected near Dornburg, Germany (+51°00′52.00″, +11°38′17.00″), on *Populus maximowiczii* × *Populus nigra*. The beetles were lab-reared at 18 ± 2°C in light (16 h) and 13 ± 2°C in darkness (8 h).

### *RNA extraction and cDNA synthesis*

Different *P. cochleariae* larval tissues (fat body, gut and Malpighian tubules) were dissected under the microscope and stored in 100 $\mu$L lysis-buffer (Life Technologies, Carlsbad, USA) with the addition of 1 $\mu$L ExpressArt NucleoGuard (Amp Tec GmbH, Germany) at −80°C until needed. Total RNA from stored tissues was isolated with the RNAqueous®-Micro Kit (Life Technologies, Carlsbad, USA) according to the manufacturer's instruction. The RNA from whole larvae of *P. cochleariae* and *C. populi* was isolated with the RNAqueous kit (Life Technologies, USA). All RNA samples were stored at −80°C after extraction. For RNA samples used for quantitative real-time PCR (qPCR), the genomic DNA was digested by DNase I (Thermo Fisher Scientific, Langenselbold, Germany) prior to cDNA synthesis.

For cDNA-synthesis, a total of 400 ng RNA was used together with 1 $\mu$L SuperScript III Reverse Transcriptase (Life Technologies, USA) and 0.5 $\mu$g/$\mu$L Oligo(dT)$_{12–18}$ Primers (Life Technologies, USA) per 20 $\mu$L reaction. The cDNA template from *P. cochleariae* fat body for 3′ rapid amplification of cDNA ends (3′ RACE) was synthesized according to the manual from SMARTer RACE 5′/3′ Kit (Takara Bio, Inc. Mountain View, CA, USA). All cDNA templates were stored at −20°C after synthesis.

### *Analysis of the expressional profile of P450s in different tissues*

qPCR was performed to analyze the expression pattern of *CYP347W1* in different tissues (fat body, gut and Malpighian tubules) with Bio-Rad CFX96 real time PCR detection system (Bio-Rad Laboratories, Munich, Germany). Each RT-qPCR reaction (20 $\mu$L final volume) contained 10 $\mu$L Brilliant III SYBR Green qPCR Master Mix (Agilent Technologies, Waldbronn, Germany), 0.6 $\mu$L of cDNA, and 0.2 $\mu$L each of forward and reverse gene-specific primers (Table S1, working concentration 10 $\mu$mol/L). An initial incubation at 95°C for 3 min was conducted, followed by 40 cycles at 95°C for 10 s, 60°C for 20 s, and at 72°C for 30 s. Three technical replicates were applied to three biological replicates. Technical replicates with a Cq difference >0.5 were excluded. Elongation factors 1a (*Pc EF1a*) and the eukaryotic translation initiation factor 4a (*Pc eIF4a*) were chosen as reference genes for normalization. Primers were designed by primer3plus (http://www.bioinformatics.nl/cgibin/primer3plus/primer3plus.cgi), all primer sequences can be found in the Table S1. All assays were performed according to the MIQE-guidelines (Bustin *et al*., 2009).

### *Silencing of CYP347W1 by RNAi*

The full-length open reading frame of *CYP347W1* was analyzed by siFi 21 (https://sourceforge.net/projects/sifi21/) for off-target prediction using a threshold value of at least 21 consecutive nucleotides. The unique fragments (>400 bp) were used to design double strand (dsRNA) primers (Table S1) and all dsRNA fragments (including the ds*eGFP* control) were synthesized using the MEGAscript RNAi Kit (Thermo Fisher Scientific, Langenselbold, Germany). After purification, the dsRNA was diluted in 0.9% NaCl solution and adjusted to a concentration of 2 $\mu$g/$\mu$L. Second instar *P. cochleariae*

larvae were anesthetized on ice prior to injection. For each larva, 100 ng dsRNA was injected into the hemolymph under the microscope with a glass capillary. Larvae injected with only dsRNA targeting *eGFP* were taken as the control group. After injection, the larvae were transferred into insect rearing cups and were kept under normal rearing conditions.

### *Hemolymph collection*

Larval hemolymph was collected by glass capillaries (i.d.: 0.28 mm, o.d.: 0.78 mm, length: 100 mm; Hirschmann, Eberstadt, Germany) and then transferred to a 200 $\mu$L Eppendorf tube. The weight of the hemolymph was obtained by weighing empty and filled tubes with hemolymph. All samples were stored at −20°C until needed.

### *Identification of compound 1, compound 2, 3-NPA and β-alanine by HPLC-MS and gas chromatography-mass spectrometry (GC-MS)*

For the detection of compounds 1 and 2, the stored larval hemolymph samples were dissolved in 50 $\mu$L 90% ethanol supplemented with 4 $\mu$L $^{13}C_6$-labeled compounds 1 and 2 authentic standard mixture. The internal standard mixture was prepared in a volume ratio of 25 : 10 : 1 for $^{13}C_6$-labeled compound 1 (3.736 mmol/L in $ddH_2O$), $^{13}C_6$-labeled compound 2 (2.034 mmol/L in $ddH_2O$) and Paraoxon (18.8 mmol/L in ethanol; Merck KGaA, Darmstadt, Germany), respectively (Becker *et al*., 2013, 2015). Analysis was carried out using an Agilent HP1100 HPLC-MS system equipped with a LiChrospher® 100 RP-18 (5 $\mu$m) LiChroCART® 250-4 column (Merck KGaA, Darmstadt, Germany) connected to a Finnigan LTQ MS detector (Thermo Electron Corp, Dreieich, Germany). The detector operated in the atmospheric pressure chemical ionization (APCI) mode (vaporizer temperature: 500°C, capillary temperature: 300°C). The program was set by following the description stated by Pauls *et al*. (2016). For identification, the mass-to-charge ratio (*m*/*z*) at 292 for compound 1 and *m*/*z* at 393 for compound 2, and the *m*/*z* plus 6, respectively, for the corresponding $^{13}C_6$-labeled internal standards were used. The peak areas were calculated by Thermo Xcalibur Quan Brower implemented in the Xcalibur software (Thermo Fisher Scientific, Langenselbold, Germany). The relative amount of compounds 1 and 2 present in each $\mu$g hemolymph was calculated against the $^{13}C_6$-labeled internal standards that were spiked in the solvent.

To detect 3-NPA and $\beta$-alanine with GC-MS, the solvent of both extracts from the fat body and the enzyme assays were dried under nitrogen flow at room temperature for 30 min. 3-NPA and $\beta$-alanine were derivatized with 50 $\mu$L N-methyl-N-tert-butyldimethylsilyl-trifluoroacetamide (MBDSTFA) at 70°C for 30 min. After the derivatization, the samples were dried again under nitrogen flow and redissolved in 100 $\mu$L ethyl acetate. The supernatants were transferred to GC vials for measurement. One microliter was subjected to GC-MS analysis [ThermoQuest ISQ mass spectrometer LT system (quadrupole) equipped with a Phenomenex ZB-5-W/Guard-column, 25 m (10 m Guardian precolumn) × 0.25 mm, film thickness: 0.25 $\mu$m]. The detector operated in electron ionization (EI) mode. The program was as follows: 45°C (2 min), 10°C per minute to 200°C, 30°C per minute to 300°C (1 min). The inlet temperature was 220°C and the transfer line was at 280°C. 3-NPA and $\beta$-alanine were identified by the comparison of the retention time and mass spectra to the authentic standards.

### *Construction of the recombinant plasmids*

The full-length open reading frame sequence of *CYP347W1* was amplified with the Phusion High-Fidelity DNA Polymerase (Life Technologies, Carlsbad, CA, USA) and the corresponding primers (Table S1), afterward, the full length was verified by sequencing. The right sequence containing the stop codon was subcloned into the pFastBac Dual expression vector directly with primers appended with NotI and HindIII restriction enzyme cleavage sites named as CYP347W1_NotI_F and CYP347W1_HindIII_R. To facilitate the detection of the recombinant protein with western blot, the constructs without the stop codon were subcloned in parallel. To achieve this, *CYP347W1* without the stop codon was first subcloned into the pcDNA™3.1D/V5-His-TOPO expression vector with primers CYP347W1_pc_F and CYP347W1_pc_R. Then the third pair of primers designed based on the pcDNA™3.1D/V5-His-TOPO expression vector was used to amplify *CYP347W1* with the C-terminal overhang of the V5 epitope and His tag. The obtained fragment was further subcloned into the pFastBac Dual expression vector. A *C. populi* cytochrome P450 reductase (CPR) was cloned and was subjected to similar operations as mentioned above (Fu *et al*., 2019). Both *CYP347W1* and *CPR* inserts were cloned downstream of and controlled by the PH promoter in the pFastBac™ Dual vector. The recombinant positive plasmids were analyzed and verified by PCR and sequencing

and were stored at −20°C. For the sequences of all the primers mentioned here, see Table S1.

*Heterologous expression*

Recombinant *CYP347W1*/*CPR* was coexpressed in Sf9 insect cells using the Bac-to-Bac baculovirus expression system. First, the purified pFastBac Dual plasmid containing either *CYP347W1* or *CPR* was transformed into DH10Bac™ *E. coli* for transposition into the bacmid. Colonies containing the recombinant bacmids were identified by blue/white selection according to the protocol. And the positive recombinant bacmids were further verified by PCR and sequencing. Afterward, the postive bacmids were transfected to the Sf9 insect cells to produce the recombinant baculovirus stocks (Thermo Fisher Scientific, Langenselbold, Germany). Supernatant was harvested and the titer of the recombinant baculoviral stock was determined following the manufacturer's instructions by plaque assay. Sf9 cells were then coinfected with recombinant baculoviral stocks P2 expressing *CYP347W1* and *CPR* with a MOI of 1 and 0.1, respectively. Sf9 cells were maintained at 27°C with Sf-900 II SFM medium (Life Technologies, Carlsbad, CA, USA), supplemented with 2.5 $\mu$g/mL hemin and 0.3% (vol/vol) fetal bovine serum (Atlas Biologicals, Fort Collins, CO, USA). After 72 h, cells were harvested for microsome isolation according to the methods described by Joussen *et al*. (2012). The microsomes were aliquoted and stored at −80°C after determining the concentration with the Quick Start Bradford Protein Assay Kit (Bio-Rad Laboratories, Munich, Germany).

*SDS PAGE and Western Blot*

Microsomal fractions containing *CYP347W1* and *CPR*, fused with a V5 epitope tag and a His-tag were denatured by incubation at 70°C for 5 min and followed by SDS PAGE. Afterward, membrane proteins were blotted onto a polyvinylidene difluoride (PVDF) membrane (Trans-Blot® Turbo™ Mini PVDF Transfer Pack; Bio-Rad) with a Bio-Rad blotting system. The membrane was blocked first in blocking buffer (5% (wt/vol) nonfat dry milk in Tris-buffered saline with Tween-20 (TBST) buffer) for 1 h and then incubated overnight with Anti-V5-HRP antibodies (1 : 10 000; Thermo Fisher Scientific, Langenselbold, Germany) in another blocking buffer (0.25 % [wt/vol] nonfat dry milk in TBST buffer) at 4°C. The membrane was washed three times with TBST buffer prior to incubation (1 min) with enhanced chemiluminescence (ECL) solution (Thermo Fisher Scientific, Langenselbold, Germany). Amersham Hyperfilm ECL X-ray film (GE Healthcare, Boston, USA) was exposed to the PVDF membrane prior to developing the film.

*Enzyme assays*

The microsomal fractions with the recombinant CYP347W1 and CPR protein lacking the V5 epitope and His-tag were used for the enzyme assays. The assay was performed in 50 $\mu$L volume containing 25 $\mu$g microsomal proteins in 20 mmol/L potassium phosphate buffer (pH 7.5), 200 $\mu$mol/L $\beta$-alanine and 1 mmol/L NADPH. The same assay without NADPH served as the negative control. For the empty control, 25 $\mu$g microsomal proteins from cells that were infected with the recombinant CPR virus only were used. After incubation at 30°C for 30 min, the reaction was stopped by freeze and thaw cycles.

*Homology modeling*

The 3D-protein structure homology modeling of CYP347W1 was performed with YASARA, Version 17.12.24 (Krieger *et al*., 2009; Krieger & Vriend, 2014). After search for templates in the protein database, 10 appropriate X-ray templates were found (pdb-codes: 5VCC, 5VCD, 5VEU, 6C93, 3NA1, 6C94, 4I91, 3MDM, 5UFG, 4ZV8) (Berman *et al*., 2000). Altogether 88 models including alternative sequence alignments for the 10 templates was generated by YASARA. The quality of all homology models was evaluated using PROCHECK and ProSA II (Laskowski *et al*., 1993; Sippl, 1990, 1993). The model based on the X-ray structure of, 5VEU, scored at –1.178, was the best, for the longest amino acid chain modeled with a sequence identity of 33.9% and a sequence similarity of 53.8% (BLOSUM62 score is >0). Finally, a hybrid model was automatically generated which included better scored short alternative loop structures from the other models. This hybrid model was subsequently refined with the md-refinement tool of YASARA (20 simulated annealing runs for 500 ps). A model with excellent quality was achieved, based on the Ramachandran plot, with 91.7% residues being in the most favoured region and two outliers only in loop regions. All other stereochemical parameters were also checked; the ProSA II energy graphs were in negative range (windows size = 40) and the calculated *z*-scores was in the range of natively folded proteins.

One hundred docking positions of $\beta$-Ala-CoA were generated by docking to the active site close to heme using MOE 2018.01 (https://www.chemcomp.com/). From

several alternative docking positions, two of them exhibited a close distance between the amino ($\beta$-Ala)-methyl group with the peroxide bound to heme. To check stability of the arrangement a final md-refinement run was performed.

## Results

### *P. cochleariae fat body is the biosynthetic site for both compound 1 and 2*

A previous study has shown that activities of UDP-glucosyltransferase for the production of compound 1 and of ATP/CoA-dependent enzyme(s) to incorporate the 3-NPA moiety into compound 2 were detected in the fat body of Chrysomelina beetles, indicating that both compound 1 and 2 are synthesized in the *P. cochleariae* fat body (Becker *et al*., 2016). To validate this assumption, the *P. cochleariae* crude fat body extract was first subjected to HPLC-MS analysis. As shown in Figure 2A, both compound 1 and 2 were detected by comparing the retention times and mass spectra to the synthesized $^{13}C_6$-labeled authentic standards. Additionally, GC-MS analysis revealed a peak corresponding to the silylated 3-NPA also present in the fat body extract (Fig. 2B). The presence of both compounds 1-, 2-, and 3-NPA in the fat body supports the assumption that the biosynthesis of these compounds takes place in the fat body.

### *CYP347W1 is an abundant enzyme in the fat body of P. cochleariae larvae*

As we are interested in CYPs that are involved in biosynthesis for both compound 1 and compound 2, we focused on those that are highly expressed specifically in the fat body. While screening the expression pattern of putative P450 candidates in *P. cochleariae* larvae (Fu *et al*., 2019), a contig referred as C480, and here named as *CYP347W1* according to the cytochrome P450 nomenclature committee, drew our attention. It displayed a surprisingly high transcriptional level exclusively in the fat body, exceeding that in the gut and Malpighian tubules by around 294-fold and 138-fold, respectively (Fig. 3). Compared to other known P450s, the deduced amino acid sequence of *CYP347W1* exhibits the highest amino acid identity (54%) to one functional uncharacterized P450 (accession number: XM_023169053.1) from the Colorado potato beetle *Leptinotarsa decemlineata*. Among other hits that share more than 40% amino acid identities based on the family concept of CYPs, none of them has been functionally characterized. In the genetically closely related sequestering leaf beetles, *C. populi*, which also produces compounds 1 and 2, we have identified a homolog of *CYP347W1* (namely comp619) sharing 90.9% amino acid identity. This homolog exhibited a similar transcriptional profile to *CYP347W1*, being highly expressed in the larval fat body. Altogether, the feature of fat body specific accumulation of a group of highly conserved CYPs among different Chrysomelinae species indicate their special and important roles in the fat body's metabolism.

### *CYP347W1 is involved in 3-NPA production in P. cochleariae larvae*

To address the question of whether *CYP347W1* is involved in the production of compounds 1 and 2, we examined the knockdown effect of *CYP347W1* on the larval ability to produce both compounds. As shown in Fig. 4A, the relative expression level of *CYP347W1* was quite stable at selected sampling days in those larvae injected with ds*eGFP*; while in ds*CYP347W1* injection group, the transcriptional level of *CYP347W1* has dropped significantly to only 2% of that in ds*eGFP* treated group on the 3rd day after injection. Afterward, the downregulation pattern of *CYP347W1* remained stable for the following sampling days in the ds*CYP347W1* treated group, indicating that the RNAi effect had been triggered and the *CYP347W1* gene had been knocked down successfully in ds*CYP347W1* injected larvae. In addition, knocking down *CYP347W1* did not affect the larval body weight gain trends in both ds*eGFP* and ds*CYP347W1* treated groups (Fig. 4B).

Since both compound 1 and 2 accumulate in the larval hemolymph, the relative amounts of both compounds in the hemolymph from larvae injected with ds*CYP347W1* and ds*eGFP* were compared. As shown in Fig. 4C, on the 3rd and 5th day, the relative amount of compound 1 in hemolymph from *CYP347W1* knockdown larvae was always slightly higher than that in larvae from the ds*eGFP* treated group. Remarkably, on the 7th day after injection, compound 1 in the ds*CYP347W1* treated group was significantly more abundant than that in larvae injected with ds*eGFP*. On the 9th day, the observed statistically significant difference was counterbalanced by the slight decrease of compound 1 in *CYP347W1* knock down group. In contrast, compared to the *dseGFP*-treated group, the relative amount of compound 2 in the ds*CYP347W1* treated group decreased significantly and steadily from around 80% on the 3rd day after injection to about only 2% on the 9th day after injection (Fig. 4D). Additionally, we tested the presence of 3-NPA in the fat body

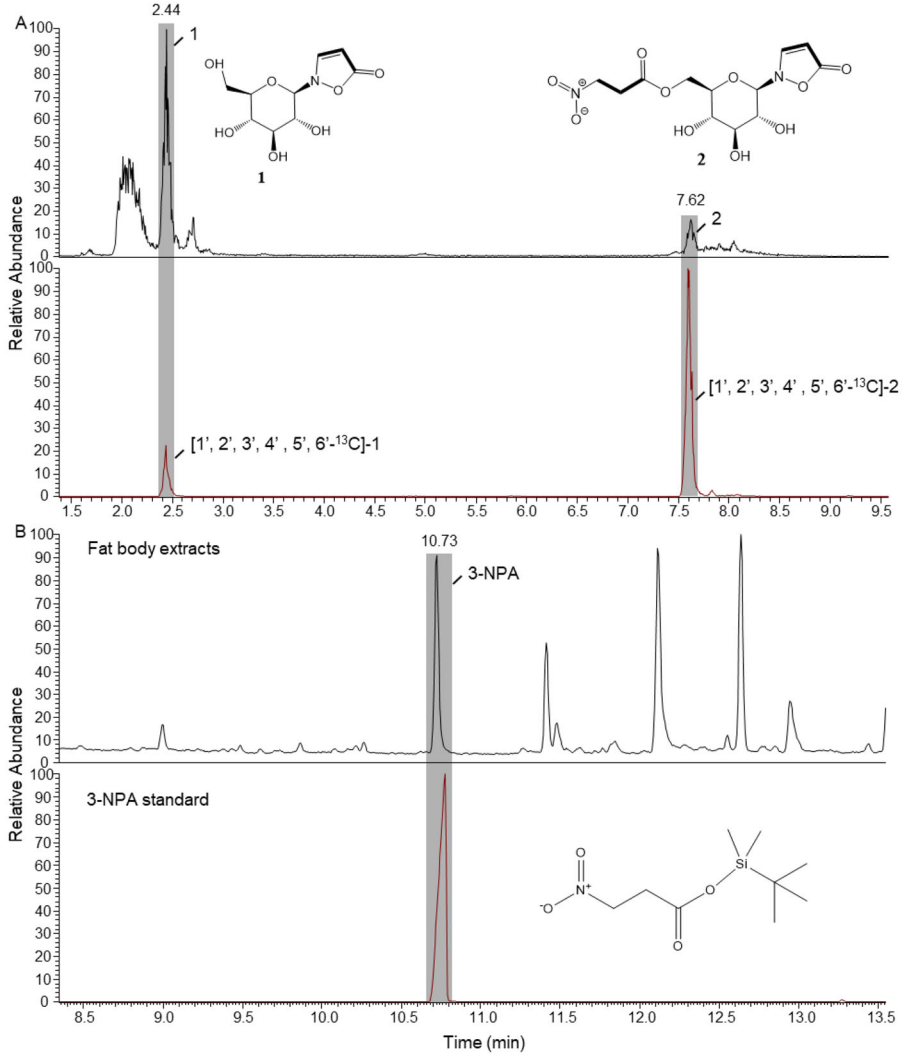


**Fig. 2** Validation of the presence of compound 1 (RT: 2.44 min, *m*/*z* 292), compound 2 (RT: 7.62 min, *m*/*z* 392) and silylated 3-NPA (RT: 10.73 min) in the fat body extracts of *P. cochleariae*. (A) The HPLC chromatogram for compound 1 and 2, and (B) the GC chromatogram of silylated 3-NPA. The identification of both compounds 1 and 2 in the fat body extract was assigned based on the comparison of the retention time and mass spectrum to the synthetic $^{13}$C-labeled authentic standards with *m*/*z* at 298 for compound 1 and *m*/*z* at 398 for compound 2 (Figs. S1 and S2). Marked signals correspond to $[M+HCOOH]^-$ ions. 3-NPA was silylated with MBDSTFA, and the identification of silylated 3-NPA in the fat body extract was assigned based on the comparison of the retention time and mass spectrum to the authentic standard (Fig. S3).

extracts from larvae in both ds*CYP347W1* and ds*eGFP* treated groups on the 7th day after injection. No 3-NPA was detected in the larvae injected with ds*CYP347W1* compared to the ones receiving ds*eGFP*, but a minor accumulation of $\beta$-alanine was observed in the *CYP347W1* knockdown group (Fig. 5). To sum up, these results revealed that *CYP347W1* is an important enzyme for the production of the 3-NPA moiety of compound 2. Moreover, it is conceivable that *P. cochleariae* recruits an enzyme independent of *CYP347W1* for the biosynthesis of the isoxazolin-5-one heterocycle moiety, though both 3-NPA and isoxazolin-5-one are derived from the common precusor $\beta$-alanine.

To determine, if *CYP347W1* can use free $\beta$-alanine for the synthesis of 3-NPA, CYP347W1 was coexpressed with the cytochrome P450 reductase CPR in Sf9 insect cells using the baculovirus expression system successfully (Fig. S5). Pilot experiments by using free $\beta$-alanine, however, showed no obvious enzymatic activity. Homology modeling revealed that CYP347W1 is likely to

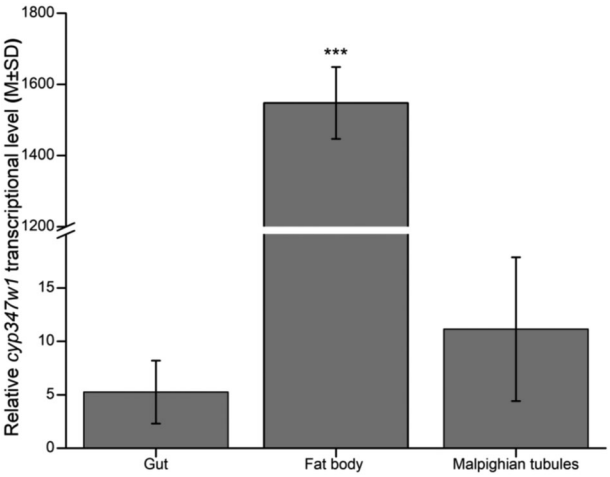


**Fig. 3** Transcriptional abundance ($2^{-\Delta Cq}$) of *CYP347W1* in different larval tissues detected by qPCR ($n = 3$–4). Two-tailed student's *t*-test for unequal variances was used to value the significance levels. Asterisks represent significant differences in fat body compared to gut and Malpighian tubules (***$p < 0.001$).

accept $\beta$-alanine-CoA ester as a substrate rather than free $\beta$-alanine (Fig. 6A). As shown in Fig. 6B, the amino group of $\beta$-alanine-CoA is coordinated close to the peroxide of heme of CYP347W1 (magenta carbon atoms) by the formation of a salt bridge with D295. $\beta$-alanine-CoA is stabilized by the formation of salt bridges between K106 and the diphosphate moiety of CoA, and also between K72 and the monophosphate of CoA. Additionally, some hydrophobic interactions with F103, F117, F210, V361, and L480 with short hydrophobic moieties of CoA helps to stabilize the entire docking arrangement.

### *Correlation between the CYP347W1 transcriptional abundance and the amount of compounds 1 and 2 throughout P. cochleariae life cycle*

Previous studies have shown that compounds 1 and 2 are present in all the life stages of *P. cochleariae* (Matsuda & Sugawara, 1980; Pasteels *et al*., 1986; Becker *et al*., 2016; Pauls *et al*., 2016). However, whether the beetles from different life stages (egg, larva, pupa, and adult) share the same biosynthetic enzymatic repertoire for the production of compounds 1 and 2 is unknown. To investigate this aspect, the relationship between the transcriptional abundance of *CYP347W1* from *P. cochleariae* in different life stages and the corresponding amounts of compounds 1 and 2 was observed. As shown in Fig. 7A, there was no expression of *CYP347W1* in the eggs, and the gene started to express after hatching of the eggs. In the larval stage, there existed a significant transcriptional upregulation of *CYP347W1* from the first instar to the second instar larvae, and the transcriptional level remained stable for the following stages of the life cycles. In terms of the amounts of compound 1 and compound 2, our results are in agreement with the previous studies, emphasizing the ubiquitous presence of both compounds in all life stages (see Fig. 7B). Specifically, the relative amounts of both compounds were similar in the eggs, the first and second instar larvae. From Fig. 7C, we can see the larva's bodyweight increased rapidly during the transition from the second instar to the third instar. Along with the weight gain, both compound 1 and compound 2 showed a similar abruptly increasing pattern; afterward, the abundance of both compounds remained relatively stable (Fig. 7B). This coincreasing pattern between the body weight and the total amount of both compounds 1 and 2, respectively, revealed that these two compounds are present in the beetle at relatively stable concentrations (Fig. 7D). Compound 1 was at a concentration of about 10 nmol per mg body weight, while compound 2 seemed to have a higher relative concertation in eggs and first instar larvae (15 nmol per mg body weight). The concentration of compound 2 decreased slightly to around 10 nmol per mg body weight in the second instar and was maintained afterward. To sum up, our results indicated that, except for the eggs, *P. cochleariae* larvae, pupae, and adults share the same enzyme, CYP347W1, for 3-NPA production and the eggs can not synthesize compounds 1 and 2 de novo.

## Discussion

Chrysomelina leaf beetles use the noxious 3-NPA that is stored as a nontoxic and enzymatically hydrolysable ester (compound 2) to fend off their enemies (Becker *et al*., 2016). In search of the enzymes that are involved in compound 2 biosynthesis, we identified a cytochrome P450 CYP347W1. By suppressing the expression of *CYP347W1* using RNAi, a significant decrease in the concentration of compound 2 along with an increase in the concentration of compound 1 in the hemolymph were detected. Furthermore, a depletion of 3-NPA was also observed in the fat body extracts from *CYP347W1* knockdown larvae, when compared to the ds*eGFP* treated group. These results conclusively showed that *CYP347W1* is involved in the production of the toxic 3-NPA moiety of the defense compound 2 in Chrysomelina leaf beetles. The minor accumulation of $\beta$-alanine in *CYP347W1* knockdown *P. cochleariae* larvae supported the conclusion that the backbone of 3-NPA originated

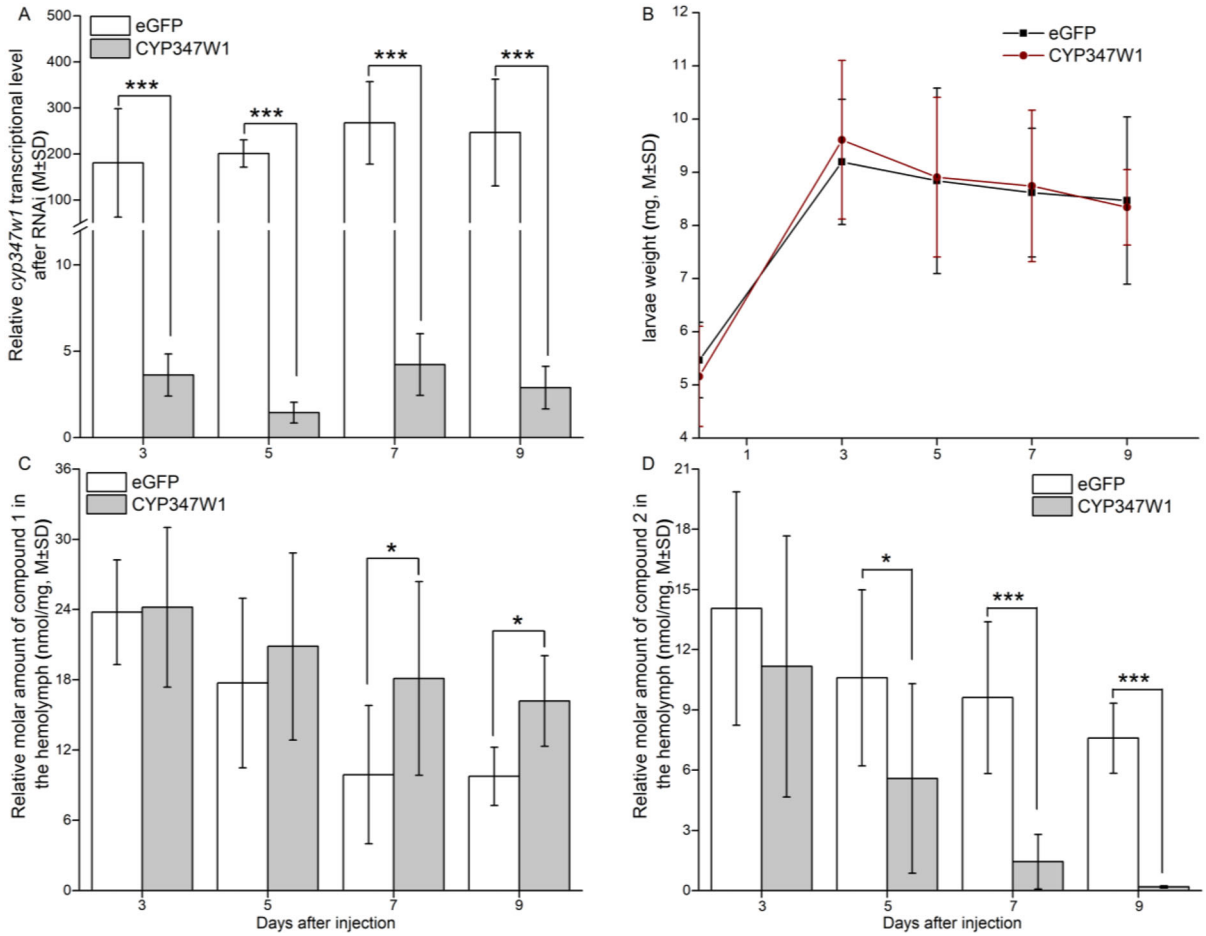


**Fig. 4** Timeline of the knockdown effects of *CYP347W1*. (A) The body weight gain of *P. cochleariae* larvae was not influenced by RNAi ($n \geq 10$). (B) The transcriptional level of *CYP347W1* in the whole larva ($n = 3$). (C)–(D) The relative amounts of compound 1 and 2 measured in the hemolymph after dsRNA injection ($n \geq 10$). Each larva was taken as a biological replicate. Two-tailed student's *t*-test for equal variances was used to value the significance levels, and the asterisks represent significant differences in CYP347W1 knockdown larvae compared to dseGFP injected control larvae (*$P < 0.05$, ***$P < 0.001$).

from $\beta$-alanine (Becker *et al*., 2016). However, in vitro enzyme assays showed that *CYP347W1* had no activity toward free $\beta$-alanine. But homology modeling indicated that $\beta$-alanine-CoA can fit into CYP347W1's active center. To validate whether CYP347W1 can accept $\beta$-alanine-CoA as substrate,the synthesis of $\beta$-alanine-CoA is essential.

Although 3-NPA differs from isoxazolin-5-one in the oxidative state of the nitrogen atom and chain arrangment, a previous study has shown that both compounds are derived from the common precursor, $\beta$-alanine, in Chrysomelina leaf beetles, as shown in Figure 1 (Becker *et al*., 2016). The observed significant increase of compound 1 detected in the larvae from *CYP347W1* knockdown group further indicated that, despite of the same origin, different enzymes are used for the biosynthesis of 3-NPA and isoxazoline-5-one. Based on the RNAi screening experiments, it is proposed that the mustard leaf beetles *P. cochleariae* rather recruited N-oxygenase(s) from other protein families than the P450 superfamily for the consecutive oxidation from $\beta$-alanine to isoxazolin-5-one.

In addition to the Chrysomelina leaf beetles, trials to elucidate the biosynthesis of 3-NPA in other organisms have also been made. For example, in fungi, 3-NPA was shown to derive from L-aspartic acid instead of $\beta$-alanine (Baxter *et al*., 1992; Chomeheon *et al*., 2005). And L-aspartic acid was converted to 3-NPA by a flavin-dependent oxidoreductase FzmM with L-nitrosuccinate as the intermediate in the fosfazinomycin producing

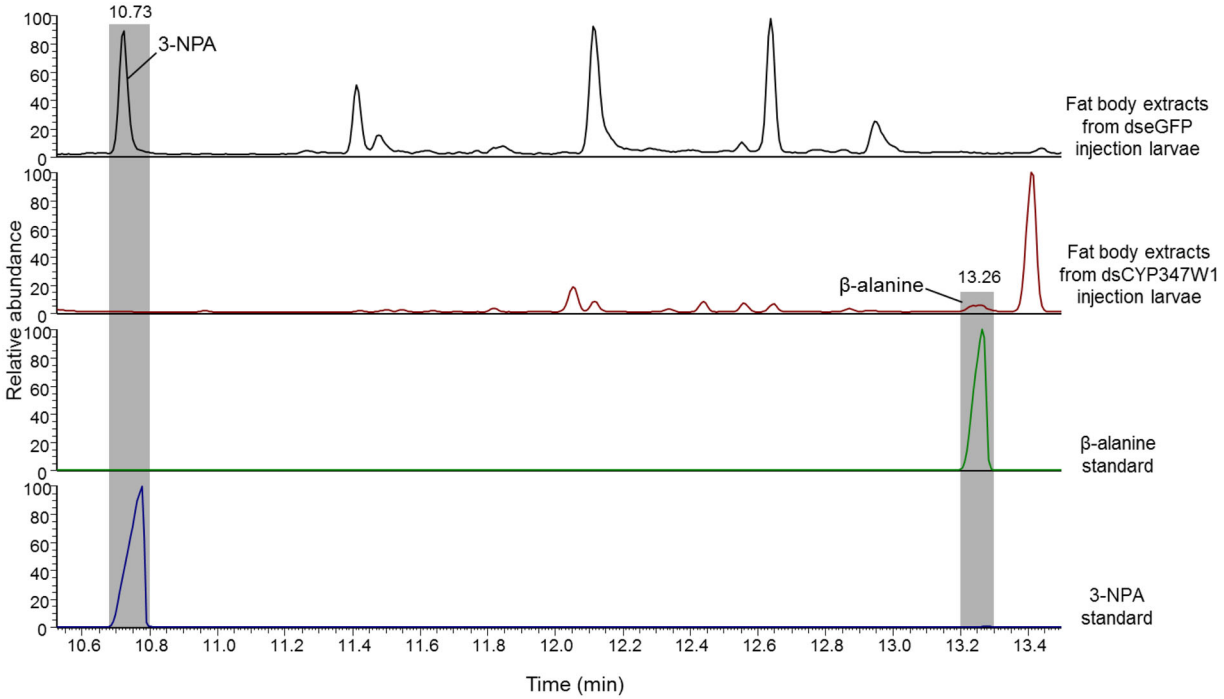


**Fig. 5** GC-MS total ion chromatograms to detect the presence of 3-NPA (RT: 10.73 min) and $\beta$-alanine (RT: 13.26) in the fat body of *P. cochleariae* on the seventh day after RNAi. The samples were silylated with MBDSTFA. The identification of silylated 3-NPA and $\beta$-alanine in the fat body extract was assigned based on the comparisons of the retention time and mass spectrum to the authentic standards (Figs. S3 and S4).

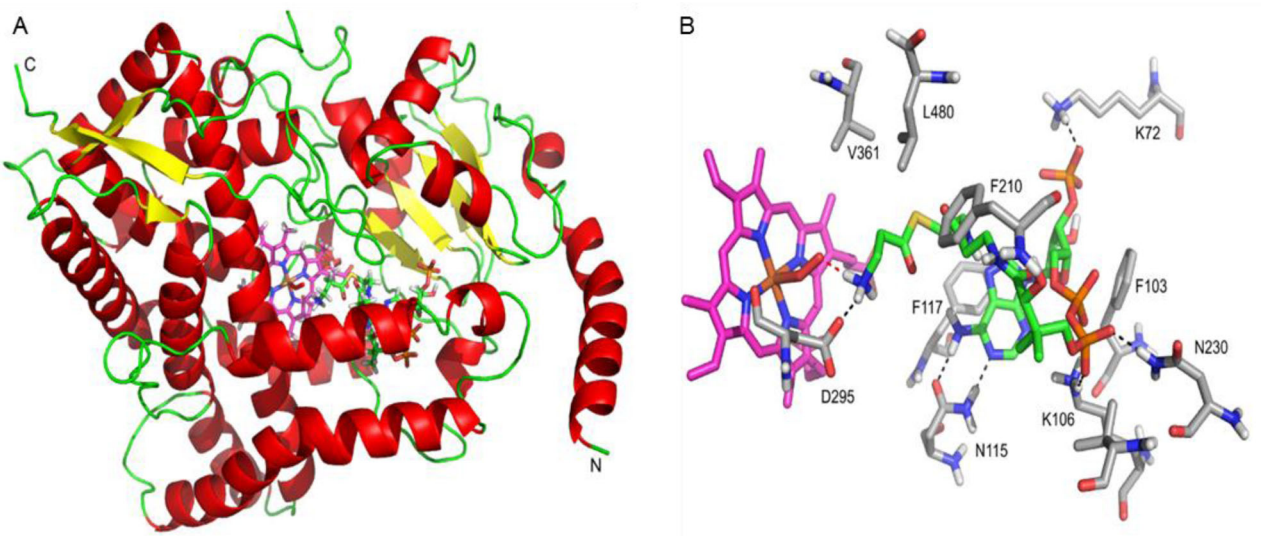


**Fig. 6** Homology modeling of $\beta$-alanine-CoA (green carbon atoms) in the active center of CYP347W1. (A) Tertiary structure of CYP347W1 with docked $\beta$-alanine-CoA (green carbon atoms). The amino group of $\beta$-alanine-CoA is close to the peroxide of heme (magenta carbon atoms). (B) Binding site of $\beta$-alanine-CoA (green carbon atoms) in the active site of CYP347W1. The amino group of $\beta$-alanine-CoA is coordinated close to the peroxide of heme of CYP347W1 (magenta carbon atoms) by the formation of a salt bridge with D295. $\beta$-alanine-CoA is stabilized by the formation of salt bridges between K106 and the diphosphate moiety of CoA, and between K72 and the monophosphate of CoA. Additionally, some hydrophobic interactions with F103, F117, F210, V361, and L480 with short hydrophobic moieties of CoA help to stabilize the entire docking arrangement.

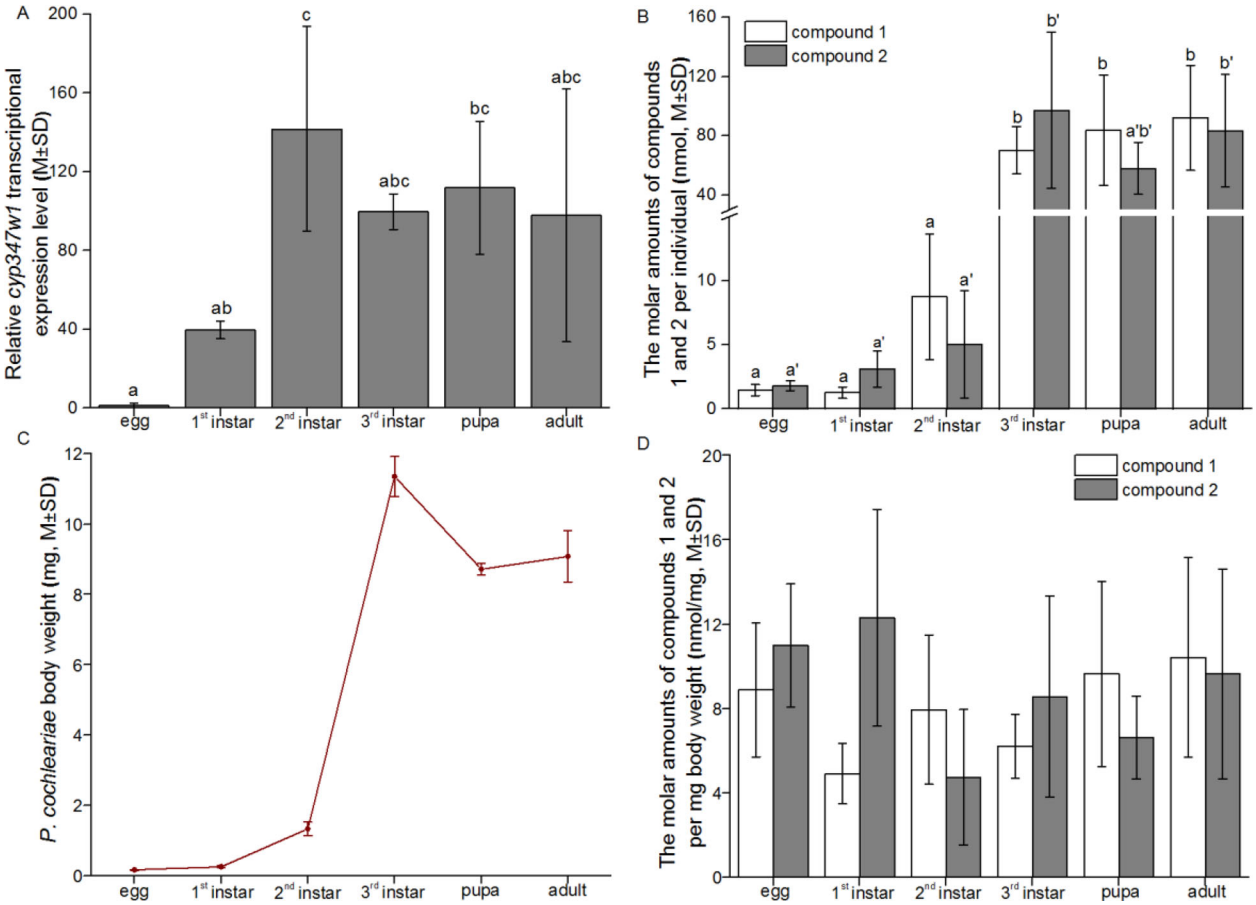


**Fig. 7** The transcriptional abundance of *CYP347W1* and the amounts of compounds 1 and 2 in different life stages of *P. cochleariae*. (A) The transcriptional level of CYP347W1 in *P. cochleariae* across the life cycle. (B) The total amount of compounds 1 and 2 in each individual. (C) The weight of each *P. cochleariae* individual from different life stages. (D) The relative amounts of compounds 1 and 2, which is normalized against the weight of *P. cochleariae* from different life stages. Statistically significant differences among different life stages were determined by one-way ANOVA using Tukey's post hoc test. Each life stage contained five individuals and each larva was a biological replicate. Samples designated with the same letters indicate there were no significant differences.

streptomyces (Huang *et al*., 2016). In Chrysomelina leaf beetles, L-aspartic acid did not participate in 3-NPA production, as indicated by the stable isotope labeling experiments (Becker *et al*., 2016). Our RNAi results further showed knocking down *CYP347W1* led to almost complete loss of 3-NPA production on the seventh day after injection. Consistent with the previous L-aspartic acid labeling assays, our results consolidated the exclusion of endophytic fungi's roles in 3-NPA production in Chrysomelina leaf beetles. Apart from fungi and Chrysomelina leaf beetles, 3-NPA is also widely present in the leguminous plants (Hipkin *et al*., 2004; Ossedryver *et al*., 2013). Radioactive labeling experiments in *Indigofera spicata* (creeping indigo) indicated the plant uses malonic acid as the precursor for 3-NPA production (Candlish *et al*., 1969). However, considering the low $^{14}C$ incorporation rate (0.02%–0.08%) and the presence of 3-NPA producing endophytic fungi in some leguminous plants (Chomeheon *et al*., 2005), it is unclear whether the 3-NPA in these plants was produced by the plants or by the endophytic fungi. Moreover, the possibility of utilizing $\beta$-alanine as a precursor for 3-NPA production by those leguminous plants, as found in the leaf beetles, can also not be excluded. In terms of the origins of 3-NPA, the $\beta$-alanine and P450-dependent synthetic strategy for 3-NPA production in Chrysomelina leaf beetles is quite different from the aspartic acid and flavin-dependent oxidoreductase-based mechanism found in fungi, and also from the malonate acid-derived biosynthesis proposed in leguminous plants. This discovery further indicates that 3-NPA biosynthesis evolved independently in these organisms.

The use of 3-NPA and its derivatives by different organisms to protect themselves against unfavorable conditions such as predation can be a powerful chemical defensive strategy. The feature of being a suidcide inhibitor of ATP production, however, necessitates the 3-NPA producing organisms to develop detoxifying mechanisms to avoid self-intoxication (Ludolph *et al*., 2015). Apart from storing 3-NPA as the corresponding glucosides, the leguminous plants and fungi are able to convert 3-NPA to oxidized inorganic nitrogen such as nitrate and nitrite using 3-NPA oxidase (Porter & Bright, 1987; Hipkin *et al*., 1999). In the Chrysomelina leaf beetles, compound 1 was considered as the detoxifyed carrier for the toxic free 3-NPA. This hypothesis was supported by the finding that compound 1 can conjugate two free 3-NPAs in the adult secretions collected from some Japanese Chrysomelid beetles (Sugeno & Matsuda, 2002). Our observation of the slightly higher amount of compound 1 as a result of 3-NPA downregulation due to *CYP347W1* knockdown also supports compound 1's role of being a 3-NPA carrier. Pauls *et al*. (2016) showed that *P. cochleariae* larvae can tolerate up to 300 ng 3-NPA per mg body weight. As shown in Fig. 7D, compound 1 was at a relative stable level throught the beeltes' life cycle. The relatively high abundance of compound 1 may partly explain the 3-NPA tolerance in Chrysomelina leaf beetles. In addition, a study have also showed that the generalist herbivore *Spodoptera littoralis*, can excrete 3-NPA into the feces in the form of amino acid-conjugated amides (Novoselov *et al*., 2015). A similar 3-NPA detoxifying mechanism was also observed in the grasshopper *Melanoplus bivittatus* (Majak *et al*., 1998). It remains unknown, whether Chrysomelina beetles are also able to detoxify 3-NPA by forming of amino acid amides in addition to forming ester compound 2.

## Acknowledgments

We sincerely thank Toni Krause, Jana Pieper, and Sarah Bauer for their help in heterologous protein expression. The authors would also like to express their gratitude to David Nelson (University of Tennessee) for help with P450 nomenclature. This work was financially supported by the Max Planck Society and the China Scholarship Council (grant number 201406300098).

## Author Contributions

N.F., A.B., and W.B. designed the research. N.F. performed the experiments and analyzed the data, assisted by T.B., M.K. W.Br. did the homology modeling. N.F., T.B., W.Br., M.K, A.B., and W.B. wrote the article. All authors read and approved the manuscript.

## Disclosure

The authors declare that they have no conflicts of interest.

## References

Anderson, R.C., Majak, W., Rassmussen, M.A., Callaway, T.R., Beier, R.C., Nisbet, D.J. *et al*. (2005) Toxicity and metabolism of the conjugates of 3-nitropropanol and 3-nitropropionic acid in forages poisonous to livestock. *Journal of Agricultural and Food Chemistry*, 53, 2344–2350.

Baxter, R.L. and Greenwood, S.L. (1986) Application of the $^{18}O$ isotope shift in $^{15}N$ N.M.R. spectra to a biosynthetic problem: experimental evidence for the origin of the nitro group oxygen atoms of 3-nitropropanoic acid. *Journal of the Chemical Society-Chemical Communications*, 2, 175–176.

Baxter, R.L., Hanley, A.B., Chan, H.W.S., Greenwood, S.L., Abbot, E.M., McFarlane, I.J. *et al*. (1992) Fungal biosynthesis of 3-nitropropanoic acid. *Journal of the Chemical Society, Perkin Transactions 1*, 19, 2495–2502.

Baxter, R.L., Smith, S.L., Martin, J.R. and Hanley, A.B. (1994) The fungal biosynthesis of 3-nitropropionic acid: is the decarboxylation of L-nitrosuccinate an enzymatic reaction? *Journal of the Chemical Society, Perkin Transactions 1*, 16, 2297–2299.

Becker, T., Görls, H., Pauls, G., Wedekind, R., Kai, M., von Reuß, S. and Boland, W. (2013) Synthesis of isoxazolin-5-one glucosides by a cascade reaction. *The Journal of Organic Chemistry*, 78(24), 12779–12783.

Becker, T., Kartikeya, P., Paetz, C., von Reuß, S. and Boland, W. (2015) Synthesis and photosensitivity of isoxazolin-5-one glycosides. *Organic & Biomolecular Chemistry*, 13(13), 4025–4030.

Becker, T., Ploss, K. and Boland, W. (2016) Biosynthesis of isoxazolin-5-one and 3-nitropropanoic acid containing glucosides in juvenile Chrysomelina. *Organic and Biomolecular Chemistry*, 14(26), 6274–6280.

Berman, H.M., Westbrook, J., Feng, Z., Gilliland, G., Bhat, T.N., Weissig, H. *et al*. (2000) The protein data bank. *Nucleic Acids Research*, 28, 235–242.

Bustin, S.A., Benes, V., Garson, J.A., Hellemans, J., Huggett, J., Kubista, M. *et al*. (2009) The MIQE guidelines: minimum information for publication of quantitative real-time PCR experiments. *Clinical Chemistry*, 55, 611–622.

Candlish, E., La Croix, L.J. and Unrau, A.M. (1969) Biosynthesis of 3-nitropropionic acid in creeping indigo (*Indigofera spicata*). *Biochemistry*, 8, 182–186.

Chomeheon, P., Wiyakrutta, S., Sriubolmas, N., Ngamrojanavanich, N., Isarangkul, D. and Kittakoop, P. (2005) 3-nitropropionic acid (3-NPA), a potent antimycobacterial agent from endophytic fungi: is 3-NPA in some plants produced by endophytes? *Journal of Natural Products*, 68, 1103–1105.

Fu, N., Yang, Z.L., Pauchet, Y., Paetz, C., Brandt, W., Boland, W. *et al*. (2019) A cytochrome P450 from the mustard leaf beetles hydroxylates geraniol, a key step in iridoid biosynthesis. *Insect Biochemistry and Molecular Biology*, 113, 103212.

Greule, A., Stok, J.E., De Voss, J.J. and Cryle, M.J. (2018) Unrivalled diversity: the many roles and reactions of bacterial cytochromes P450 in secondary metabolism. *Natural Product Reports*, 35, 757–791.

Guengerich, F.P. (2001) Common and uncommon cytochrome P450 reactions related to metabolism and chemical toxicity. *Chemical Research in Toxicology*, 14, 611–650.

Hamilton B.F., Gould D.H. and Gustine D.L. (2000) History of 3-nitropropionic acid. *Mitochondrial Inhibitors and Neurodegenerative Disorders* (eds. P.R. Sanberg, H. Nishino & C.V. Borlongan). Contemporary Neuroscience, Humana Press, Totowa, NJ.

Hipkin, C.R., Salem, M.A., Simpson, D. and Wainwright, S.J. (1999) 3-nitropropionic acid oxidase from horseshoe vetch (*Hippocrepis comosa*): a novel plant enzyme. *Biochemical Journal*, 340, 491–495.

Hipkin, C.R., Simpson, D.J., Wainwright, S.J. and Salem, M.A. (2004) Nitrification by plants that also fix nitrogen. *Nature*, 430(6995), 98–101.

Huang, L.S., Sun, G., Cobessi, D., Wang, A., Shen, J.T., Tung, E.Y. *et al*. (2006) 3-nitropropionic acid is a suicide inhibitor of mitochondrial respiration that upon oxidation by complex II forms a covalent adduct with a catalytic-base Arginine in the active site of the enzyme. *Journal of Biological Chemistry*, 281, 5965–5972.

Huang, Z., Wang, K.K.A. and van der Donk W.A. (2016) New insights into the biosynthesis of fosfazinomycin. *Chemical Science*, 7, 5219–5223.

James, L.F., Hartley, W.J., Williams, M.C., and Van Kampen K.R. (1980) Field and experimental studies in cattle and sheep poisoned by nitro-bearing Astragalus or their toxins. *American Journal of Veterinary Research*, 41, 377–382.

Joussen, N., Agnolet, S., Lorenz, S., Schone, S.E., Ellinger, R., Schneider, B. *et al*. (2012) Resistance of Australian *Helicoverpa armigera* to fenvalerate is due to the chimeric P450 enzyme CYP337B3. *Proceedings of the National Academy of Sciences USA*, 109, 15206–15211.

Krieger, E., Joo, K., Lee, J., Lee, J., Raman, S., Thompson, J. *et al*. (2009) Improving physical realism, stereochemistry, and side-chain accuracy in homology modeling: four approaches that performed well in CASP8. *Proteins*, 77 Suppl 9, 114–122.

Krieger, E. and Vriend, G. (2014) YASARA View—molecular graphics for all devices—from smartphones to workstations. *Bioinformatics*, 30, 2981–2982.

Lamb, D.C., Lei, L., Warrilow, A.G.S., Lepesheva, G.I., Mullins, J.G.L., Waterman, M.R. *et al*. (2009) The first virally encoded cytochrome P450. *Journal of Virology*, 83, 8266–8269.

Lamb, D.C. and Waterman, M.R. (2013) Unusual properties of the cytochrome P450 superfamily. *Philosophical transactions of the Royal Society of London Series B, Biological sciences*, 368(1612), 20120434.

Laskowski, R.A., MacArthur, M.W., Moss, D.S. and Thornton, J.M. (1993) PROCHECK: a program to check the stereochemical quality of protein structures. *Journal of Applied Crystallography*, 26(2), 283–291.

Liu, X., Luo, X. and Hu, W. (1992) Studies on the epidemiology and etiology of moldy sugarcane poisoning in China. *Biomedical and Environmental Sciences*, 5, 161–177.

Ludolph, A.C., He, F., Spencer, P.S., Hammerstad, J. and Sabri, M. (2015) 3-Nitropropionic acid—exogenous animal neurotoxin and possible human striatal toxin. *Canadian Journal of Neurological Sciences*, 18, 492–498.

Majak, W.M., Johnson, D.L. and Benn, M.H. (1998) Detoxification of 3-nitropropionic acid and karakin by melanopline grasshoppers. *Phytochemistry*, 49, 419–422.

Matsuda, K. and Sugawara, F. (1980) Defensive secretion of Chrysomelid larvae *Chrysomela vigintipunctata* costella (Marseul), *C. populi* L. and *Gastrolina depressa* BALY (Coleoptera: Chrysomelidae). *Applied Entomology and Zoology*, 15, 316–320.

Montellano, P.R.O.D. (2010) Hydrocarbon hydroxylation by cytochrome P450 enzymes. *Chemical Reviews*, 110, 932–947.

Novoselov, A., Becker, T., Pauls, G., von Reuss, S. H. and Boland, W. (2015) *Spodoptera littoralis* detoxifies neurotoxic 3-nitropropanoic acid by conjugation with amino acids. *Insect Biochemistry and Molecular Biology*, 63, 97–103.

Ossedryver, S.M., Baldwin, G.I., Stone, B.M., McKenzie, R.A., van Eps, A.W., Murray, S. *et al*. (2013) *Indigofera spicata* (creeping indigo) poisoning of three ponies. *Australian Veterinary Journal*, 91, 143–149.

Pasteels, J., Daloze, D. and Rowell-Rahier, M. (1986) Chemical defence in Chrysomelid eggs and neonate larvae. *Physiological Entomology*, 11, 29–37.

Pauls, G., Becker, T., Rahfeld, P., Gretscher, R.R., Paetz, C., Pasteels, J. *et al*. (2016) Two defensive lines in juvenile leaf beetles: esters of 3-nitropropionic acid in the hemolymph and aposematic warning. *Journal of Chemical Ecology*, 42, 240–248.

Porter, D.J. and Bright, H.J. (1987) Propionate-3-nitronate oxidase from *Penicillium atrovenetum* is a flavoprotein which initiates the autoxidation of its substrate by $O_2$. *Journal of Biological Chemistry*, 262, 14428–14434.

Randoux, T., Braekman, J.C., Daloze, D. and Pasteels, J.M. (1991) *De novo* biosynthesis of 3-isoxazolin-5-one and 3-nitropropanoic acid derivatives in *Chrysomela tremulae*. *The Science of Nature*, 78, 313–314.

Robert, W. and Christian, H. (2007) Biosynthesis of nitro compounds. *ChemBioChem*, 8, 973–977.

Sippl, M. (1990) Calculation of conformational ensembles from potentials of mena force. *Journal of Molecular Biology*, 213(4), 859–883.

Sippl, M. (1993) Recognition of errors in three-dimensional structures of proteins. *Proteins: Structure, Function, and Genetics*, 17(4), 355–362.

Su, Y.F., Lu, M., Yang, F.Y., Li, C. Z., Di, L.Z., Wu, D. *et al*. (2008) Six new glucose esters of 3-nitropropanoic acid from *Indigofera kirilowii*. *Fitoterapia*, 79, 451–455.

Sugeno, W. and Matsuda K. (2002) Adult secretions of four Japanese Chrysomelinae (Coleoptera: Chrysomelidae). *Applied Entomology and Zoology*, 37(1), 191–197.

Tunez, I., Tasset, I., Perez-De La Cruz, V. and Santamaria, A. (2010) 3-Nitropropionic acid as a tool to study the mechanisms involved in Huntington's disease: past, present and future. *Molecules*, 15, 878–916.

Williams, M.C. and James, L.F. (1975) Toxicity of nitro-containing astragalus to sheep and chicks. *Journal of Range Management*, 28, 260–263.

Williams, M.C., van Kampen, K.R. and Norris, F.A. (1969) Timber milkvetch poisoning in chickens, rabbits, and cattle. *American Journal of Veterinary Research*, 30, 2185–2190.

Manuscript received April 12, 2021
Final version received June 5, 2021
Accepted June 15, 2021

## Supporting Information

Additional supporting information may be found online in the Supporting Information section at the end of the article.

**Fig. S1**. Mass spectra of isoxazoline-5-one-glucoside (mass: 292) and $^{13}C_6$-labeled isoxazoline-5-one-glucoside (mass: 298). The marked signals correspond to $[M+HCOOH]^-$ ions.

**Fig. S2**. Mass spectra of 3-NPA-conjugated isoxazoline-5-one-glucoside ester (mass: 392) and $^{13}C_6$-labeled 3-NPA-conjugated isoxazoline-5-one-glucoside ester (mass: 398) standards. The marked signals correspond to $[M+HCOOH]^-$ ions.

**Fig. S3**. Mass spectra of the MBDSTFA silylated 3-NPA. Mass spectrum of the authentic standard of 3-NPA (up) and of the peak corresponding to 3-NPA detected in the larval fat body extracts in Figure 3 (down). Based on the retention time and the high similarity with the mass spectrum of the authentic standard, the peak was identified as 3-NPA.

**Fig. S4**. Mass spectra of the MBDSTFA silylated $\beta$-alanine. Mass spectrum of the authentic standard of $\beta$-alanine (up) and of the peak corresponding to $\beta$-alanine detected in the fat body extracts from larvae in *CYP347W1* knockdown group in Figure 3 (down). Based on the retention time and the high similarity with the mass spectrum of the authentic standard, the peak was identified as $\beta$-alanine.

**Fig. S5**. Western blot to detect the heterologous expressed recombinant CYP347W1/CPR proteins with the Anti-V5-HRP antibody. Microsome was prepared from Sf9 cells that were cotransfected with recombinant baculoviral vectors expressing CYP347W1 and CPR that fused to V5 epitope and His-tag. The observed molecular mass agreed with the prediction from their corresponding amino acid sequences.

**Table S1**. Primers used for the research.